Direct evidence for mode-specific vibrational energy relaxation from quantum time-dependent perturbation theory. II. The ν_4 and ν_7 modes of iron-protoporphyrin IX and iron porphine

Yong Zhang[a] and John E. Straub[b]
Department of Chemistry, Boston University, Boston, Massachusetts 02215, USA

(Received 4 December 2008; accepted 2 February 2009; published online 5 March 2009)

The mode-specific vibrational energy relaxation (VER) of the iron-protoporphyrin IX (the heme) was studied using a non-Markovian time-dependent perturbation theory at the UB3LYP/6-31G(*d*) level. The derived VER time constants of the excited ν_4 and ν_7 modes, 1.2 ± 0.1 and 2.1 ± 0.1 ps, respectively, agree well with previous experimental results for MbCO (1.1 ± 0.6 ps for the ν_4 mode and 1.9 ± 0.6 ps for the ν_7 mode). The energy transfer pathways from the excited ν_4 and ν_7 modes were identified. The different symmetries of the ν_4 and ν_7 modes are reflected in distinct relaxation pathways. No direct energy transfer between the ν_4 and ν_7 modes was observed. The overtone of the ~ 350 cm^{-1} iron out-of-plane γ_7 mode was observed to be strongly coupled to the ν_7 mode and essential to its relaxation. The two isopropionate side chains of the heme were found to play an essential role in the VER mechanism for both ν_4 and ν_7 modes, providing the mode-specific level explanation to previous observations. Comparison of the results for VER in iron porphine (FeP) to results for the imidazole-ligated porphine model (FeP-Im) demonstrates that the axial Im ligand has little effect on the ν_4 or ν_7 mode relaxation processes. By considering the VER process as a multistep reaction and the third order Fermi resonance parameters the reaction rate constants, the VER kinetics of FeP was examined by solving the master equation. © *2009 American Institute of Physics*. [DOI: 10.1063/1.3086080]

I. INTRODUCTION

Efficient dissipation of excess energy following chemical reaction is essential to the maintenance of protein structure and the enhancement of protein function. In myoglobin (Mb) or hemoglobin (Hb), ligand dissociation can occur when the ligand-heme complex absorbs a visible or UV photon. Photodissociation can cause vibrational excitation of the ligand, the heme, and the surrounding residues.[1,2] The identification of the time scales and mechanisms of vibrational energy relaxation (VER) that follow such events is an essential component of any detailed understanding of the ultrafast conformational changes associated with protein function. As a result, this topic has been the focus of intense experimental and theoretical studies for over 30 years.[3–24]

Anfinrud *et al.* observed that the heme cooling process in Mb following ligand photodissociation follows a single-exponential decay with a time constant of 6.2 ± 0.5 ps.[25] A similar heme cooling rate with time constant ~ 5.9 ps was derived from molecular dynamics simulations by Sagnella and Straub.[26] Bu and Straub further explored the heme cooling mechanism through direct classical molecular dynamics simulations of myoglobin mutants and variants designed to disrupt the heme protein coupling by replacing the ligating proximal His93 with Gly or the heme solvent coupling by deleting the acidic heme side chains. In H93G mutated myoglobin, a single-exponential process of heme cooling with a time constant of 5.9 ps was observed, identical to the heme relaxation in the native myoglobin.[27] In the Mb variant, in which the two isopropionate side chains are replaced by aliphatic hydrogens, the relaxation time constant increased to 8.8 ps. The strong interaction between the isopropionate side chains and solvent was conjectured to be the dominant pathway for heme cooling.[27] This conjecture was supported by subsequent experimental studies on the H93G mutant and similar modified heme variants of myoglobin.[28–30] The detailed interaction between the heme isopropionate side chains and solvent was examined recently through classical molecular dynamics simulation of myoglobin in various polar and nonpolar solvents.[31]

Using time-resolved resonance Raman spectroscopy, Kitagawa and co-workers monitored the mode-specific behavior of heme vibrational relaxation following ligand dissociation.[32–35] The decay time constants of the highly excited ν_4 and ν_7 modes following the ligand photodissociation reaction were found to be 1.1 ± 0.6 and 1.9 ± 0.6 ps, respectively, implying a thermal decay of the heme within 2 ps,[34,35] faster than the heme cooling rate reported previously. Similar mode-specific properties were observed for metalloporphyrins models.[36–41]

In previous work,[42] using the time-dependent perturbation theory and density functional theory, we studied the mode-specific VER in a five-coordinate ferrous iron porphyrin model (FeP-Im), designed to mimic the photodissociated heme moiety in myoglobin. An imidazole ligand was included in the model but no side chains were involved. The

[a]Present address: Department of Chemistry, University of Utah, Salt Lake City, UT 84112. Electronic mail: zhangy@hec.utah.edu.
[b]Author to whom correspondence should be addressed. Electronic mail: straub@bu.edu.

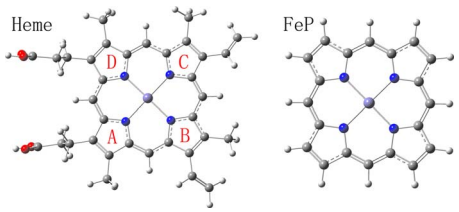

FIG. 1. (Color online) Depiction of the optimized structure of iron-protoporphyrin IX (the heme) and iron porphine (FeP) at the UB3LYP/6-31G(*d*) level. The four pyrrole rings of the heme, A, B, C, and D, are labeled. The core sizes, the distances between Fe and pyrrole N atoms, were found to be 1.995 Å for the heme and 1.988 Å for FeP.

VER pathway modes identified for the relaxation of the ν_4 and ν_7 porphyrin in-plane motions are primarily porphyrin out-of-plane (oop) motions. The modes associated with imidazole ligand displacement were found to be key to the transfer of localized heme excitation to the functionally important motions underlying protein global structural change.

In this work, we extend our mode-specific study to iron-protoporphyrin IX (the heme) in an attempt to mimic the active site of myoglobin and address the role of side chains in the VER of the excited ν_4 and ν_7 modes. While axial modes are clearly of functional importance, our study indicates that axial modes do not play an essential role in the relaxation of the ν_4 and ν_7 modes.[42] Modes associated with the isopropionate side chains are of lower frequency and more directly coupled to lower frequency bath modes than the higher frequency axial modes. Our results strongly support past work suggesting an essential role of the isopropionate side chains in the relaxation process. The energy flow within the porphyrin model from the initially excited ν_4 and ν_7 modes was examined by solving a master equation leading to the conclusion that the energy equilibration within the heme is slow in comparison with the rapid relaxation of the directly excited ν_4 and ν_7 vibrations.

II. THEORY AND METHODS

A. Non-Markovian time-dependent perturbation theory

The VER rate formula[43] employed in this work is briefly summarized here. We expand the potential energy surface with respect to the normal coordinates of the system, q_S, and bath, q_α, and their frequencies, ω_S and ω_α, up to third and fourth order nonlinear couplings,

$$H = H_S + H_B - q_S \delta F + q_S^2 \delta G, \tag{1}$$

$$H_S = \frac{p_S^2}{2} + V(q_S), \tag{2}$$

$$H_B = \sum \left(\frac{p_\alpha^2}{2} + \frac{\omega_\alpha^2 q_\alpha^2}{2} \right), \tag{3}$$

$$\delta F = \sum_{\alpha,\beta} C_{S\alpha\beta}(q_\alpha q_\beta - \langle q_\alpha q_\beta \rangle), \tag{4}$$

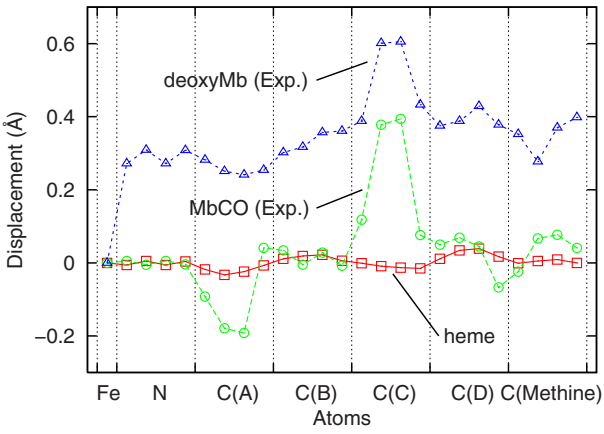

FIG. 2. (Color online) The calculated displacements of the heme porphine heavy atoms relative to the porphine plane defined by the four nitrogen atoms (with origin centered on the Fe atom) ordered as the iron, pyrrole nitrogens, pyrrole carbons (A, B, C, and D as shown in Fig. 1), and methine carbons. The displacements derived from deoxyMb and MbCO crystal structures [PDB entries 1BZP (Ref. 50) and 1MBC (Ref. 51)] are noted.

$$\delta G = \sum_{\alpha,\beta} C_{SS\alpha\beta}(q_\alpha q_\beta - \langle q_\alpha q_\beta \rangle) + \sum_\alpha C_{SS\alpha} q_\alpha, \tag{5}$$

where H_S (H_B) is the system (bath) Hamiltonian and $C_{S\alpha\beta}$ ($C_{SS\alpha\beta}$) are the third (fourth) order coupling terms. From the von Neumann–Liouville equation, a reduced density matrix for the system mode is derived using the time-dependent perturbation theory after tracing over the bath degrees of freedom. The commonly employed Markov approximation, which assumes a separation in time scales for the relaxation of the system and bath modes, is not invoked in this theory. The final VER formula is obtained as[43]

$$\begin{aligned}(\rho_S)_{00}(t) \simeq & \frac{2}{\hbar^2}\sum_{\alpha,\beta}[C_{--}^{\alpha\beta}u_t(\tilde{\omega}_S - \omega_\alpha - \omega_\beta) + C_{++}^{\alpha\beta}u_t(\tilde{\omega}_S + \omega_\alpha \\ & + \omega_\beta) + C_{+-}^{\alpha\beta}u_t(\tilde{\omega}_S - \omega_\alpha + \omega_\beta)] \\ & + \frac{2}{\hbar^2}\sum_\alpha [C_-^\alpha u_t(\tilde{\omega}_S - \omega_\alpha) + C_+^\alpha u_t(\tilde{\omega}_S + \omega_\alpha)],\end{aligned} \tag{6}$$

where the subscript of $(\rho_S)_{00}$ indicates the vibrational ground state and $u_t(\Omega)$ is defined as

$$u_t(\Omega) = \int_0^t dt' \int_0^{t'} dt'' \cos\,\Omega(t' - t'') = \frac{1 - \cos\,\Omega t}{\Omega^2}. \tag{7}$$

The coefficients, $C_{--}^{\alpha\beta}$, $C_{++}^{\alpha\beta}$, $C_{+-}^{\alpha\beta}$, C_-^α, and C_+^α, can be derived from the nonlinear coupling constants $C_{S\alpha\beta}$ and $C_{SS\alpha\beta}$.[43] When the system mode is excited to the $\nu=1$ state, VER is described by the decay of the reduced density matrix element, which is written most simply as $\rho_{11}(t) = 1 - \rho_{00}(t) \simeq \exp[-\rho_{00}(t)]$ under the cumulant approximation.

B. Simulation procedure

The four-coordinate iron porphyrin model iron-protoporphyrin IX (the heme), an iron porphyrin with eight side chains including two isopropionate groups, and the four-coordinate iron porphine (FeP), the iron porphyrin without a

TABLE I. Summary of system mode frequencies (harmonic and corrected anharmonic), the VER time constants, and the assignments studied for iron-protoporphyrin IX (the heme) and iron porphine (FeP).

Mode No.	Frequency (cm^{-1}) Harmonic (ω_S)	Frequency (cm^{-1}) Anharmonic ($\tilde{\omega}_S$)	T_1 (ps) Simulation	T_1 (ps) Expt.[a]	Assignment
		Heme			
147	1414.1	1414.0	1.2 ± 0.1	1.1 ± 0.6	ν_4
73	697.6	699.8	2.1 ± 0.1	1.9 ± 0.6	ν_7
47	351.1	353.2	17.0 ± 4.5		γ_7
		FeP			
78	1403.3	1398.2	2.1 ± 0.2		ν_4
34	739.6	735.5	3.6 ± 0.4		ν_7
15	360.8	362.1	28.6 ± 14.2		γ_7

[a]Data for carboxy Mb (Ref. 33).

side chain or ligand, were studied. Each structure was optimized to its ground triplet state[44,45] at the UB3LYP/6-31G(d) level using the GAUSSIAN03 package.[46] The "verytight" self-consistent field convergence criterion and "ultrafine" integration grid were applied in the calculation. The harmonic normal mode analysis was carried out for the optimized structure. The third and fourth order anharmonic coupling constants were calculated using a finite difference method.[47]

The system mode VER rate constants were derived by fitting the initial decay (due to the limitation of applying the cumulant approximation[48]) of the reduced density matrix $\rho_{11}(t)$ time profiles. The energy transfer pathways were identified by calculating the third order Fermi resonance parameters defined as

$$r_{S\alpha\beta} = \frac{|C_{S\alpha\beta}|}{\hbar|\tilde{\omega}_S - \omega_\alpha - \omega_\beta|}\sqrt{\frac{\hbar}{2\tilde{\omega}_S}}\sqrt{\frac{\hbar}{2\omega_\alpha}}\sqrt{\frac{\hbar}{2\omega_\beta}}, \tag{8}$$

where $\tilde{\omega}_S$ and ω_α are the frequencies of system mode and bath mode, respectively.

The geometrical overlap of the system mode S and bath modes α and β was calculated following Kidera's definition,[49]

$$G_3(S,\alpha,\beta) = \sum_{i=1}^{N_{\text{atom}}} m_i^{3/2}|\mathbf{v}_{iS}||\mathbf{v}_{i\alpha}||\mathbf{v}_{i\beta}|, \tag{9}$$

where N_{atom} is the number of atoms in the molecule, m_i is the mass of atom i, and $\mathbf{v}_{i\alpha}$ is the calculated eigenvector for mode α and atom i. Large values of G_3 imply strong spatial overlap of the system and designated bath modes.

III. RESULTS AND DISCUSSIONS

A. Calculated structure and frequencies of the heme

The optimized heme structure is depicted in Fig. 1. The displacement of each porphine core (porphyrin without the side chains) heavy atom relative to the porphyrin plane defined by the nitrogen atoms is shown in Fig. 2 along with those derived from deoxyMb and MbCO crystals [Protein Data Bank (PDB) entries 1BZP (Ref. 50) and 1MBC (Ref. 51), respectively]. The calculated porphine core is almost planar whereas the hemes in the crystal structure are distorted due to the interaction with the protein residues. Relative to the six-coordinate MbCO, the calculated heme structure is closer to the deoxyMb crystal with the exception of the iron and the carbon atoms in pyrrole C. The "core size" of the calculated heme, defined as the average distance between Fe and pyrrole N atoms, is 1.995 Å, similar to MbCO (2.005 Å) and smaller than deoxyMb (2.057 Å) (Ref. 50) due to the fact that the iron resides in the porphyrin plane.

Three modes ν_4, ν_7, and γ_7 were treated as the excited system mode independently. The calculated normal modes 147 and 73 were assigned as the ν_4 and ν_7 modes, respectively. Both ν_4 and ν_7 modes are porphyrin in-plane motions. The γ_7 mode, associated with methine wagging and Fe-oop motion, was identified as mode 47 of the heme. It was found to couple strongly with the ν_7 mode in the previous study of imidazole-ligated ferrous iron porphyrin (FeP-Im).[42] The frequencies of the three system modes, 1414.1, 697.6, and 351.1 cm^{-1}, respectively, are summarized in Table I.

B. VER of the excited system modes of the heme

Applying the time-dependent perturbation method, the VER time constants were found to be 1.2 ± 0.1 ps for the excited ν_4 mode and 2.1 ± 0.1 ps for the ν_7 mode. These values agree with the experimentally determined values for heme in MbCO following photodissociation of CO observed by Mizutani and Kitagawa (1.1 ± 0.6 ps for ν_4 mode and 1.9 ± 0.6 ps for ν_7 mode).[33] This is consistent with the fact that the heme is a relatively isolated moiety in the protein and indicates that the weak couplings through the van der Waals contacts between the heme and protein residues make a limited contribution to heme cooling. The time evolution of the excited density matrix element is shown for each mode in Fig. 3 (upper panel). The VER time constant for the excited γ_7 mode was found to be 17.0 ± 4.5 ps.

The energy transfer pathways from each excited system mode were identified by calculating the third order Fermi resonance parameters $r_{S\alpha\beta}$ using Eq. (8). The important energy transfer pathways, defined as $r_{S\alpha\beta} \geq 0.05$, are shown in Fig. 4 for the ν_4, ν_7, and γ_7 modes. Consistent with previous studies,[42,49] a large geometrical overlap was found for each

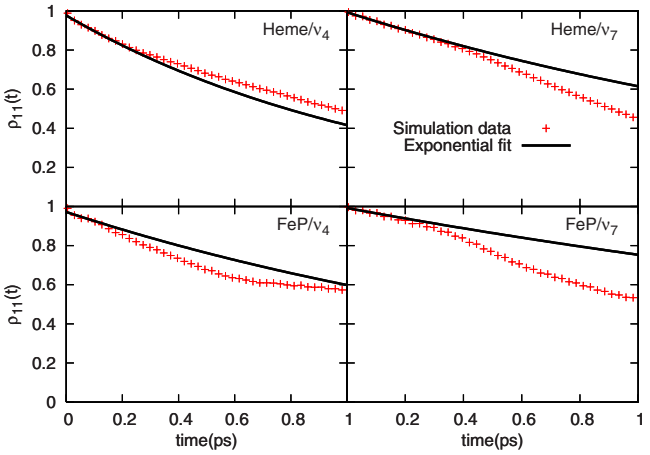

FIG. 3. (Color online) The time evolution of the initially excited density matrix element ρ_{11} for the ν_4 and ν_7 modes of the heme (upper panel) and FeP (lower panel). The simulation data are shown as points and the single-exponential fit to the initial decay is shown as a solid line. The fitted time constants are summarized in Table I. The identified important energy transfer pathways are graphically depicted in Figs. 4 and 5.

system mode and bath modes found to be essential to the energy transfer pathways. (The results are summarized in the supplemental material.[52])

By adding the side chains, the size of the model system (75 atoms) was nearly doubled over FeP-Im (46 atoms). The additional degrees of freedom and bath modes result in additional important energy transfer pathways for each excited system mode in the heme. This trend is clear for the excited γ_7 mode, which has several pathways with rather large $r_{S\alpha\beta}$ values due to strong resonance, different from FeP-Im where only one important VER pathway was identified. All bath modes were found to couple weakly with the γ_7 mode as indicated by the small third order coupling constant $C_{S\alpha\beta}$ (see Fig. 4).

Similar to FeP-Im, no direct energy transfer from the ν_4 mode to the ν_7 mode was observed in the heme. While the frequency of the ν_4 mode (1414.1 cm^{-1}) is nearly in 2:1 resonance with the ν_7 mode (697.6 cm^{-1}), allowing for potential good energy conservation; there is insufficient nonlinear coupling to facilitate that direct energy transfer pathway. The overtone of the γ_7 mode (with frequency of 351.1 cm^{-1}) was found to be an important energy transfer pathway from the excited ν_7 mode with a $r_{S\alpha\beta}$ value (1.084) that exceeds that of any other pathway. The third order Fermi resonance parameter for $\gamma_7+\gamma_7$ to ν_7 energy transfer pathway was calculated to be 0.298, larger than pathways from the excited γ_7 mode to the lower frequency bath modes, indicating that $\gamma_7+\gamma_7$ to ν_7 energy transfer pathway is essential to vibrational energy transfer in the heme.

C. VER pathways from the excited ν_4 and ν_7 modes of the heme

We focus on the essential energy transfer pathways from the excited ν_4 and ν_7 modes. For the excited ν_4 mode, 40 bath modes are involved in the important energy transfer pathways; for the excited ν_7 mode, 18 bath modes are involved. For each of these bath modes, the contribution to the norm from the porphine core, the eight side chains, and the porphine core in-plane motion were calculated. The side chain contribution was further divided into two parts, the contribution from the two isopropionate side chains and that from the other six side chains (as a whole). (The results are summarized in the supplemental material.[52]) A contribution larger than 0.5 to the norm of the porphine core indicates that the mode is "dominated" by the motion of the core region, and a contribution close to 1.0 means the mode is "localized" in that core region. While most modes are somewhat delocalized, the ν_4 mode has 0.939 contribution from the porphine core in-plane motion, and mode 5 has a 0.999 contribution from the side chains.

Table II summarizes the results for the dominant modes (with $\geq$0.5 contribution to the norm) or the localized modes ($\geq$0.8) for those modes involved in the important energy transfer pathways in ν_4 and ν_7 mode relaxations. For the 40 bath modes involved in VER from the excited ν_4 mode, 19 are dominated by the porphine core motion and 22 are dominated by the side chain motion (one bath mode, mode 118, has equal contribution from both parts). Of those modes identified with side chain motion, nine are dominated by the isopropionate groups, eight dominated by the other six side chains, and five shared by the two parts (not localized in either part). In these VER pathways from the excited ν_4 mode, six bath modes, modes 74, 79, 85, 92, 105, and 132, are localized in the porphine core. Modes 105 and 132 are mainly porphine core in-plane motions. Among others bath modes, ten modes (13, 14, 18, 21, 23, 72, 115, 135, 136, and 137) are localized in the side chains. Five of these ten modes (13, 14, 135, 136, and 137) are localized in the isopropionate groups with four of the other five modes (mode 18 is the exception) have more than 0.5 norm contribution from the isopropionate atoms. These nine modes are involved in eight important energy transfer pathways (out of 24 in total) including the 90+64 channel with the second largest $r_{S\alpha\beta}$ value (2.899, smaller than the 132+22 pathway which has better frequency resonance) and 135+18 with the third largest $r_{S\alpha\beta}$ (2.229). No mode is found to be localized in the other six side chains even when they are considered as a whole. With the exception of the 16 localized modes (6 in the core plus 10 in the side chains), most bath modes (24 out of 40) involved in the important VER pathways are shared between the porphine core and the side chain motion. In other words, they are somewhat delocalized.

For the excited ν_7 mode, five of the bath modes (35, 47, 50, 57, and 61) involved in the important energy transfer pathways are dominated by the porphine core motion. Of the bath modes, more than half (13 out of 18) are dominated by side chain motions including 4 dominated by the isopropionate groups, 2 by the other six side chains and 7 shared by all eight side chains. No mode associated with more than 0.5 contribution from the porphine core in-plane motion was found. A total of five localized bath modes are involved in the important energy transfer pathways from the excited ν_7 mode. One mode (47), the γ_7 mode, is localized in the porphine core and the other four modes (5, 24, 59, and 72) are localized in the side chains. Two modes (5 and 59) have more than 0.8 contribution to the norm from the two isopropionate groups and two others (modes 24 and 72) are domi-

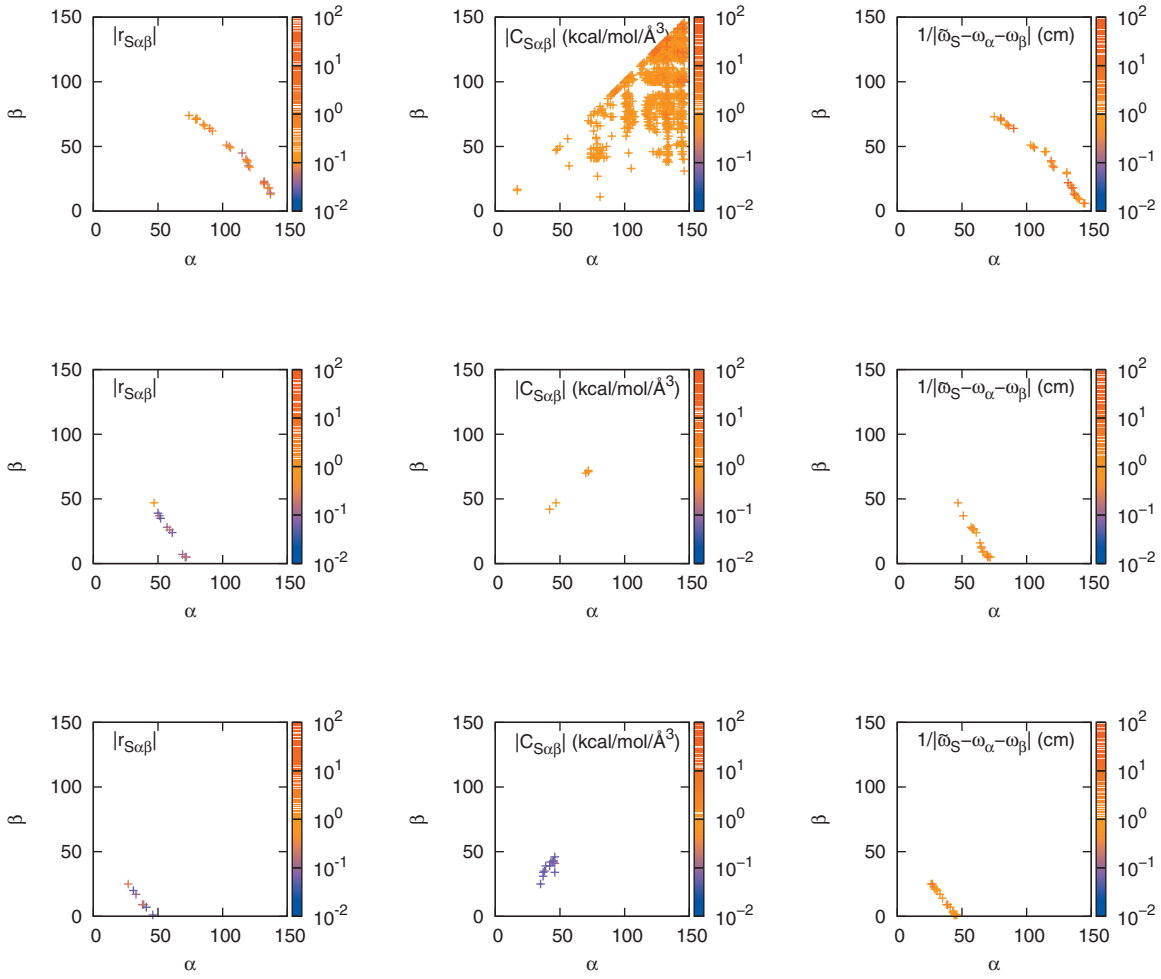

FIG. 4. (Color) The calculated third order Fermi resonance parameter $r_{S\alpha\beta}$ of the important energy transfer pathways as well as the important coupling constants $C_{S\alpha\beta}$ and the frequency resonance parameter $1/|\tilde{\omega}_S-\omega_\alpha-\omega_\beta|$ for the heme modes, from top to bottom, ν_4, ν_7, and γ_7. The x and y axes are the indices of the bath modes.

nated by the isopropionate motions. These four modes are involved in four out of ten important energy transfer pathways from the excited ν_7 mode and all have large Fermi resonance parameters. Similar to the ν_4 modes, most of the VER bath modes involve displacement of the porphine core and side chains.

As stated above, most bath modes (60.0% for ν_4 and 72.2% for ν_7) involved in the important energy transfer pathways from the excited ν_4 and ν_7 modes are delocalized motions. This may allow the energy initially deposited in the localized ν_4 and ν_7 modes to be redistributed efficiently throughout the heme or porphyrin. Our calculations indicate that the two isopropionate groups in the heme play essential and direct role in VER of the excited ν_4 and ν_7 modes. This is consistent with the conclusion of previous theoretical[26,27,31] and experimental[28–30] studies that the two isopropionate groups form the dominant pathways for directed "energy funneling" in the mechanism of rapid heme cooling in Mb.

D. Difference between ν_4 and ν_7 modes

The ν_4 and ν_7 are porphine core in-plane modes. The ν_4 mode is primarily an inner-ring breathing motion while the ν_7 mode is an outer-ring breathing motion. Our calculations indicate that the two modes share many similar VER features as well as unique relaxation pathways.

Relative to frequencies of vibration in FeP-Im, the ν_4 and ν_7 mode frequencies shift upon the addition of side chains but in opposite directions: ν_4 is blueshifted by 35 cm^{-1} while ν_7 is redshifted by 35 cm^{-1}.

Unique features were observed for the mechanism of VER from the excited ν_4 and ν_7 modes. For the excited ν_4 mode, about one-half (19 out of 40, 47.5%) of the energy accepting modes are dominated by porphine core motion, 6 of which (15.0% of total) are localized in the porphine core. In contrast, for the excited ν_7 mode, less porphine core motion was involved, including about one-quarter of the total (5 out of 18, 27.8%) dominated by the porphine core motion and only 1 mode (5.6%) localized in the porphine core. In addition, seven modes with $\geq$0.5 contribution from the porphine core in-plane motion (modes 85, 90, 105, 119, 120, 121, and 132) are involved in the important VER pathways from the excited ν_4 mode, two of which (modes 105 and 132) are localized porphine core in-plane motions. In contrast, for the excited ν_7 mode, no porphine in-plane mode was found to be essential to the VER pathway. These differences are consistent with the fact that the ν_4 mode is a mo-

TABLE II. Summary of the number of modes involved in the energy transfer pathway from the excited ν_4 and ν_7 modes of the heme as derived from B3LYP/6-31G(d) calculations. For each moiety, the contribution to the norm is noted.

Moiety	No. of bath modes	
	ν_4 mode	ν_7 mode
Total	40	18
Porphine core ≥0.5	19 (47.5%)	5 (27.8%)
All side chains ≥0.5	22 (55.0%)	13 (72.2%)
Isopropionates ≥0.5	9 (22.5%)	4 (22.2%)
Other side chains ≥0.5	8 (20.0%)	2 (11.1%)
Porphine core ≥0.8	6 (15.0%)	1 (5.6%)
All side chains ≥0.8	10 (25.0%)	4 (22.2%)
Isopropionates ≥0.8	5 (12.5%)	2 (11.1%)
Other side chains ≥0.8	0 (0.0%)	0 (0.0%)

tion associated with the porphine inner-ring atoms, mainly Fe–N and N–C stretching motions, whereas the ν_7 mode is associated with the outer-ring methine group motion. In our previous work on VER in five-coordinate FeP-Im,[42] we identified the possibility of different population excitation mechanisms for the ν_4 and ν_7 modes following ligand photodissociation in MbCO, consistent with the results of this study.

E. Role of the imidazole ligand in ν_4 and ν_7 mode VERs

To save computational expense, no axial ligand was included in the heme model employed in this work. To clarify the role of the imidazole ligand in the VER process from the excited ν_4 and ν_7 modes, we studied the VER properties of the ν_4 and ν_7 modes in iron porphine (FeP), a porphyrin model without side chains or axial ligands, and compared our results with those of our previous study of FeP-Im.

The optimized FeP has a pure planar structure (see Fig. 1). The core size was found to be 1.988 Å. The frequencies of the identified ν_4, ν_7, and γ_7 modes, 1403.3, 739.6, and 360.8 cm^{-1}, respectively, and the derived relaxation time constants are summarized in Table I. The time evolution of the excited density matrix element of the ν_4 and ν_7 modes is shown in Fig. 3 (lower panel). The relaxation of the excited ν_4 and ν_7 modes is slower than that in FeP-Im or the heme, consistent with the fact that there are fewer bath modes in FeP relative to FeP-Im and the heme.

For the excited ν_4 mode, most of the important energy transfer pathways are formed by porphine oop modes, although 2/3 of the FeP normal modes are in-plane motions (see norm contribution analysis result of each mode in the supplemental material[52]). The pathways consisting of porphine in-plane motions, 55+17, 56+16, and 57+18, have relatively small Fermi resonance parameters as a result of weak coupling. No mixed porphine oop/in-plane pathway was found to be important. For the excited ν_7 mode, only one important energy transfer pathway was identified, the overtone of the γ_7 mode. No important energy transfer pathway to the low frequency modes was observed for the excited γ_7 mode (13+4, with the largest $r_{S\alpha\beta}$ value 0.010, was shown in Fig. 5). The Fermi resonance parameter for the $\gamma_7+\gamma_7$ to ν_7 channel was found to be 0.258, indicating that it is an effective pathway essential to the mechanism of energy transfer to and from the ν_7 mode. No direct energy transfer between the ν_4 and ν_7 modes was observed.

Our results for FeP are similar to those derived for FeP-Im.[42] This is consistent with our prior study of FeP-Im, demonstrating that the imidazole-related motions form the important energy transfer pathways for the relaxation of the excited Fe oop motions but contribute little to the VER of the high frequency ν_4 and ν_7 modes.

F. Energy flow kinetics from the excited ν_4 and ν_7 modes in FeP

It has been reported previously that the heme cooling process following photodissociation of a diatomic ligand in MbCO has a time scale of 5–7 ps.[14,15,25–27,31] However, the mode-specific experimental studies on the same protein by Mizutani and co-workers revealed the VER time scales of 1–2 ps for the ν_4 and ν_7 modes.[32,33,35] One possible reason for this difference in the time scales is that the initially excited ν_4 and ν_7 modes do not dissipate their excess energy directly to the environment. Rather, our calculations indicate that the excess energy is redistributed within the heme before being fully dissipated.

We have used the third order Fermi resonance parameters $r_{S\alpha\beta}$ to explore the nature of VER pathways, where larger $r_{S\alpha\beta}$ indicates a more effective pathway. If we consider the initially excited system mode to be the reactant and the VER process a multistep reaction, the VER kinetics can be studied by solving a master equation with the third order Fermi resonance parameters as the reaction rate constants. To simplify the solution of the master equation, we only consider the transfer of energy from high frequency modes to low frequency modes or, in other words, reactions such as $A \rightarrow B+C$ with frequencies $\omega_A > \omega_B$ and $\omega_A > \omega_C$. We find

$$\frac{\partial \mathbf{P}}{\partial t} = \mathbf{RP}, \tag{10}$$

where P is the population of each mode and

$$R_{ij} = \sum_k r_{jik} \quad \text{for } j > i, \tag{11}$$

$$R_{ii} = -\sum_{j<i} \sum_{k \le j} r_{ijk}, \tag{12}$$

where r_{ijk} are the third order Fermi resonance parameters. With the boundary conditions $P(S)=1$ and $P(\alpha)=0$ at $t=0$, Eq. (10) can be solved and ideally (in the absence of a "dead end") the "reaction" will end at the lowest frequency mode.

For the optimized FeP, the third order Fermi resonance parameters r_{ijk} for each mode i were calculated from harmonic frequencies and third order anharmonic coupling constants using Eq. (8), the master equation was solved for the excited ν_4 mode, and the energy $E(i)=P(i)*\hbar\omega(i)$ was calculated for each mode i at given time t. The inclusion of

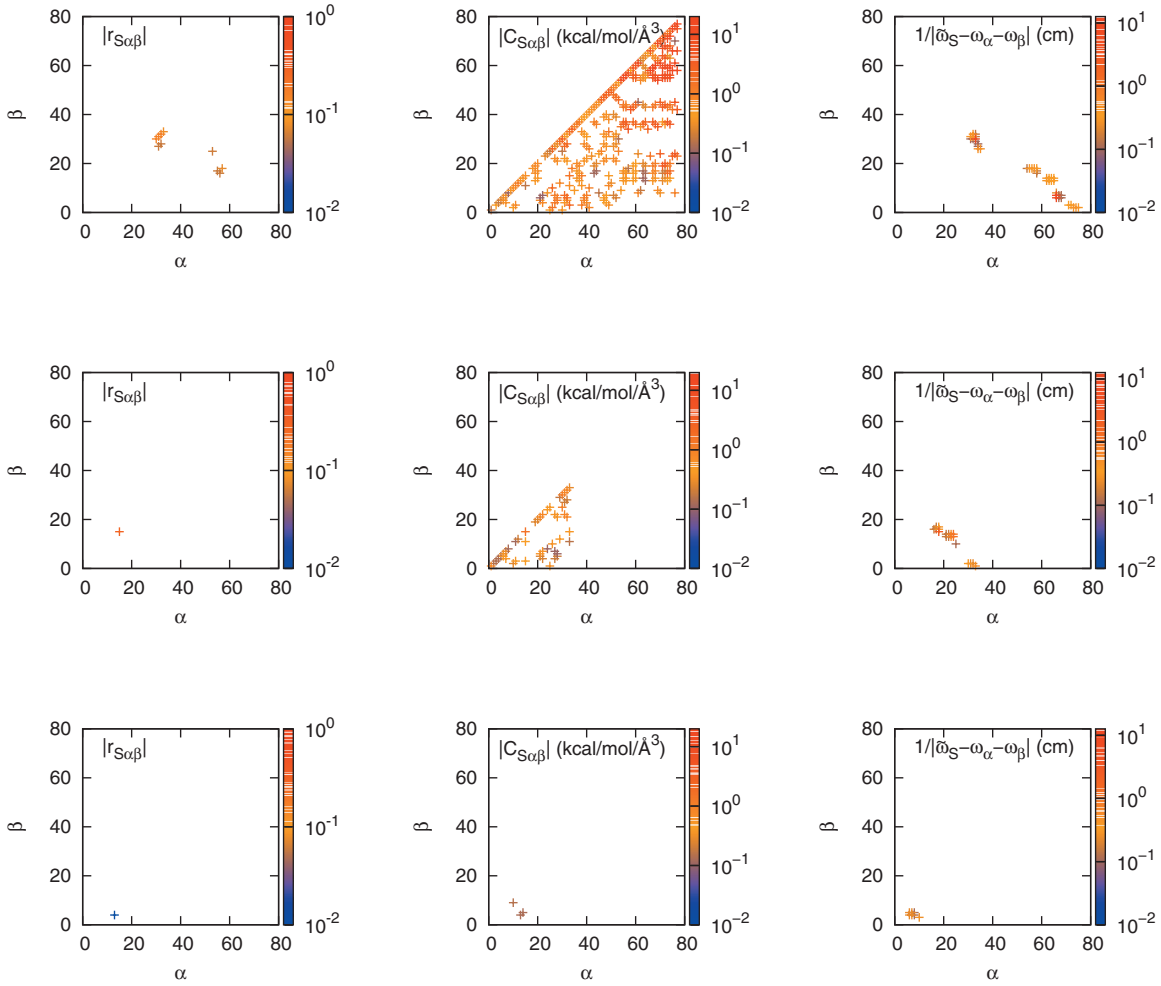

FIG. 5. (Color) The calculated third order Fermi resonance parameter $r_{S\alpha\beta}$ of the important energy transfer pathways as well as the important coupling constants $C_{S\alpha\beta}$ and the frequency resonance parameter $1/|\tilde{\omega}_S-\omega_\alpha-\omega_\beta|$ for FeP modes, from top to bottom, ν_4, ν_7, and γ_7. The x and y axes are the indices of the bath modes.

nonresonant energy transfer with significant frequency mismatch and the small frequency mismatch for the "resonant" energy transfer implies that the total energy is not exactly conserved in this approximate model that is allowed by energy uncertainty associated with finite lifetime of the bath modes. The dissipation of the "reactant," or the relaxation of the excited ν_4 mode, followed a single-exponential decay as shown in Fig. 6 (upper panel). The decay time constant was found to be $T_1=0.5$ (arbitrary time units). For most "intermediate" modes, the maximum energy was reached within $t=10$ and decayed subsequently. The maximum value and the corresponding time of a mode depend on the "rates" of population transfer to and from this mode. For example, the time evolution of the ν_7 and the γ_7 modes is shown in Fig. 6 (inset of upper panel). The ν_7 mode has a maximum energy <0.1 kcal/mol at $t=1.3$ whereas the γ_7 mode has a maximum energy ~ 0.25 kcal/mol at $t=10.2$, consistent with our observation that the relaxation from the γ_7 mode is less efficient. The time evolution of the energy of the five lowest frequency modes is shown in the lower panel of Fig. 6. At $t=1000$, a time scale much longer than the relaxation time constant of the excited ν_4 mode, equilibrium is still not reached. The explicit inclusion of protein and solvent modes is expected to facilitate relaxation to equilibrium. However, slower relaxation than that observed for the initially excited mode is expected.

When the ν_7 or γ_7 mode is treated as the system mode, similar kinetics are predicted by solving the corresponding master equation model. The relaxation time constants were found to be $T_1=1.7$ for the ν_7 mode and $T_1=24.4$ for the γ_7 mode, in agreement with the results of the time-dependent perturbation theory for the excited ν_4, ν_7, and γ_7 modes.

It has been established that the initial bond breaking process in myoglobin redistributes energy into a number of modes, with significant energy transferred to the ν_4 and ν_7 modes via mode selective coupling to the reaction coordinate.[32,53] Following that initial step, energy may be transferred to additional bath modes that are directly coupled to a limited number of accepting modes, such as the γ_7 mode, similar to the so-called regime II modes.[54,55] For this reason, the observed relaxation of the ν_4 and ν_7 modes[33] is slower than the system averaged cooling of the heme. The good agreement with experiment derived from our isolated heme model implies that there is only weak coupling due to van der Waals contacts between the heme and protein.

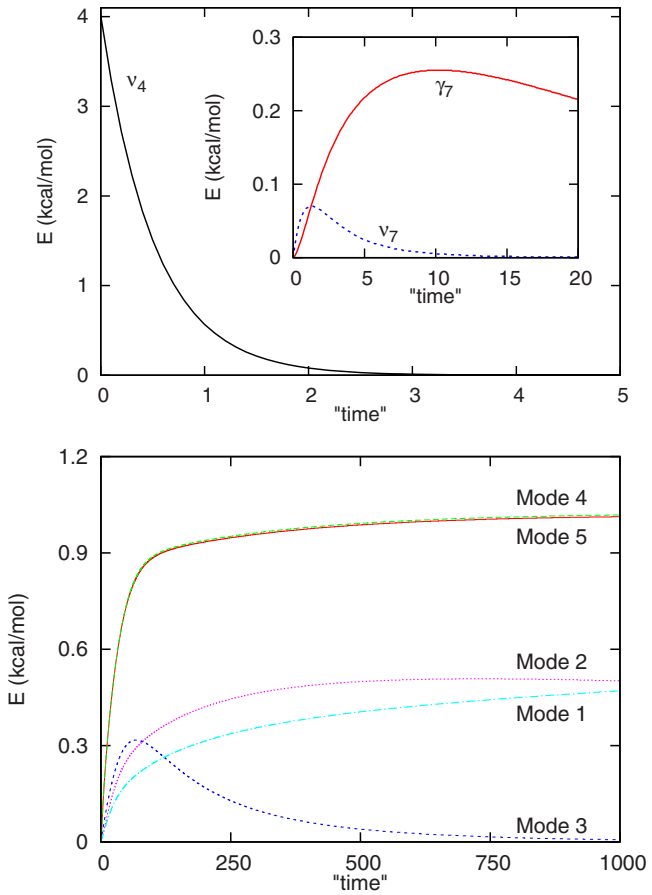

FIG. 6. (Color online) The time evolution of the energy of the ν_4 mode, ν_7 mode, γ_7 mode, and the five lowest frequency modes of FeP derived from master equation analysis with the third order Fermi resonance parameters considered to be the reaction rate constants of the multistep VER reaction from the initially excited ν_4 mode.

IV. SUMMARY AND CONCLUSIONS

The mode-specific VER of the iron-protoporphyrin IX (the heme) was studied using the time-dependent perturbation theory at the UB3LYP/6-31G(d) level. The ν_4, ν_7, and γ_7 modes of the optimized structure were assigned and treated as the system mode independently. The VER time scales and pathways were studied in detail for the excited ν_4 and ν_7 modes.

The excited ν_4 and ν_7 modes of the heme were predicted to relax with single-exponential time constants of 1.2 ± 0.1 and 2.1 ± 0.1 ps, respectively, in agreement with previous experimental results for MbCO by Mizutani and Kitagawa.[33]

The third order Fermi resonance parameters $r_{S\alpha\beta}$ were calculated for each energy transfer pathway from the excited system mode and the important relaxation pathways (with $r_{S\alpha\beta} \geq 0.05$) were identified. Similar to previous studies on FeP-Im,[42] the overtone of the γ_7 mode can effectively exchange energy with the ν_7 mode. No direct energy transfer between the ν_4 and ν_7 modes was observed.

For both the excited ν_4 and ν_7 modes, more than one-half of the energy accepting bath modes (55% for ν_4 and 72% for ν_7) are dominated by heme side chain motions. Among these bath modes, 9 out of 22 for the excited ν_4 mode and 4 out of 13 for the excited ν_7 mode are dominated by the two isopropionate side chain motions including modes localized in these groups (5 for the ν_4 mode and 2 for the ν_7 mode). Far fewer modes involved in the relaxation of ν_4 and ν_7 (eight for the ν_4 and two for the ν_7) are associated with motion of the other six side chains (as a whole). These results are consistent with the conjecture that the isopropionate side chains in the heme play an essential role in the heme cooling process following the diatomic ligand photodissociation in carbon monoxy myoglobin,[26–31] providing a deeper and more vigorous understanding of the mode-specific energy funneling mechanism responsible for heme cooling in Mb.

Bath modes associated with localized motion in the porphine core atoms are also involved in energy transfer pathways from the excited ν_4 mode. No similar coupling to core porphine in-plane modes from the ν_7 mode are observed due to the different natures of the ν_4 and ν_7 modes.

The VER properties of the ν_4 and ν_7 modes in FeP, an iron porphyrin model without side chains or axial ligands, were similarly studied and the results compared to previous results for FeP-Im. It was found that the axial ligand imidazole has little influence on the VER process of the ν_4 and ν_7 modes. Our results for the similar study of a four-coordinate heme model provide insight into the mechanism of VER for the five-coordinate heme in Mb following ligand dissociation.

The excess energy flow kinetics in FeP was examined by solving a master equation with the VER process considered as a multistep reaction and the third order Fermi resonance parameters the reaction rate constants. It was found that the subsequent relaxation is slow relative to the relaxation of the initially excited system mode, providing an explanation for the previously observed difference in relaxation time scales of heme models dependent on the exact mode of initial excitation through ligand photolysis or direct excitation.

ACKNOWLEDGMENTS

We are grateful for the generous support of this research by the National Science Foundation (Grant Nos. CHE-0316551 and CHE-0750309) and Boston University's Center for Computational Science. Our manuscript benefited from the many insightful comments and suggestions of the referees.

[1] M. C. Asplund, M. T. Zanni, and R. M. Hochstrasser, Proc. Natl. Acad. Sci. U.S.A. **97**, 8219 (2000).
[2] Y. Kholodenko, M. Volk, E. Gooding, and R. M. Hochstrasser, Chem. Phys. **259**, 71 (2000).
[3] E. Munck and P. M. Champion, Ann. N. Y. Acad. Sci. **244**, 142 (1975).
[4] J. T. Sage, C. Paxson, G. R. A. Wyllie, W. Sturhahn, S. M. Durbin, P. M. Champion, E. E. Alp, and W. R. Scheidt, J. Phys.: Condens. Matter **13**, 7707 (2001).
[5] J. T. Sage, S. M. Durbin, W. Sturhahn, D. C. Wharton, P. M. Champion, P. Hession, J. Sutter, and E. E. Alp, Phys. Rev. Lett. **86**, 4966 (2001).
[6] E. R. Henry, W. A. Eaton, and R. M. Hochstrasser, Proc. Natl. Acad. Sci. U.S.A. **83**, 8982 (1986).
[7] E. R. Henry and R. M. Hochstrasser, Proc. Natl. Acad. Sci. U.S.A. **84**, 6142 (1987).
[8] R. Elber and M. Karplus, Science **235**, 318 (1987).
[9] R. Elber and M. Karplus, J. Am. Chem. Soc. **112**, 9161 (1990).
[10] R. J. D. Miller, Annu. Rev. Phys. Chem. **42**, 581 (1991).
[11] J. E. Straub and M. Karplus, Chem. Phys. **158**, 221 (1991).
[12] H. Li, R. Elber, and J. E. Straub, J. Biol. Chem. **268**, 17908 (1993).
[13] I. Okazaki, Y. Hara, and M. Nagaoka, Chem. Phys. Lett. **337**, 151

(2001).
[14] J. W. Petrich, C. Poyart, and J. L. Martin, Biochemistry **27**, 4049 (1988).
[15] T. Lian, B. Locke, Y. Kholodenko, and R. M. Hochstrasser, J. Phys. Chem. **98**, 11648 (1994).
[16] M. Walther, V. Raicu, J. P. Ogilvie, R. Phillips, R. Kluger, and R. J. D. Miller, J. Phys. Chem. B **109**, 20605 (2005).
[17] A. M. Nagy, V. Raicu, and R. J. D. Miller, Biochim. Biophys. Acta **1749**, 148 (2005).
[18] J. R. Hill, A. Tokmakoff, K. A. Peterson, B. Sauter, D. Zimdars, D. D. Dlott, and M. D. Fayer, J. Phys. Chem. **98**, 11213 (1994).
[19] K. D. Rector, C. W. Rella, J. R. Hill, A. S. Kwok, S. G. Sligar, E. Y. P. Chien, D. D. Dlott, and M. D. Fayer, J. Phys. Chem. B **101**, 1468 (1997).
[20] K. D. Rector, J. Jiang, M. A. Berg, and M. D. Fayer, J. Phys. Chem. B **105**, 1081 (2001).
[21] I. J. Finkelstein, A. Goj, B. McClain, A. M. Massari, K. A. Merchant, R. F. Loring, and M. D. Fayer, J. Phys. Chem. B **109**, 16959 (2005).
[22] A. Xie, W. van Der Meer, L. Hoff, and R. H. Austin, Phys. Rev. Lett. **84**, 5435 (2000).
[23] H. Frauenfelder and B. H. McMahon, BioSystems **62**, 3 (2001).
[24] R. Elber and Q. H. Gibson, J. Phys. Chem. B **112**, 6147 (2008).
[25] M. Lim, T. A. Jackson, and P. A. Anfinrud, J. Phys. Chem. **100**, 12043 (1996).
[26] D. E. Sagnella and J. E. Straub, J. Phys. Chem. B **105**, 7057 (2001).
[27] L. Bu and J. E. Straub, J. Phys. Chem. B **107**, 10634 (2003).
[28] X. Ye, A. Demidov, F. Rosca, W. Wang, A. Kumar, D. Ionascu, L. Zhu, D. Barrick, D. Wharton, and P. M. Champion, J. Phys. Chem. A **107**, 8156 (2003).
[29] Y. Gao, M. Koyama, S. F. El-Mashtoly, T. Hayashi, K. Harada, Y. Mizutani, and T. Kitagawa, Chem. Phys. Lett. **429**, 239 (2006).
[30] M. Koyama, S. Neya, and Y. Mizutani, Chem. Phys. Lett. **430**, 404 (2006).
[31] Y. Zhang, H. Fujisaki, and J. E. Straub, J. Phys. Chem. B **111**, 3243 (2007).
[32] Y. Mizutani and T. Kitagawa, Science **278**, 443 (1997).
[33] Y. Mizutani and T. Kitagawa, Chem. Rec. **1**, 258 (2001).
[34] S. G. Kruglik, P. Mojzes, Y. Mizutani, T. Kitagawa, and P.-Y. Turpin, J. Phys. Chem. B **105**, 5018 (2001).
[35] T. Kitagawa, N. Haruta, and Y. Mizutani, Biopolymers **67**, 207 (2002).
[36] J. Rodriguez and D. Holten, J. Chem. Phys. **91**, 3525 (1989).
[37] J. Rodriguez, C. Kirmaier, and D. Holten, J. Chem. Phys. **94**, 6020 (1991).
[38] Y. Mizutani and T. Kitagawa, Bull. Chem. Soc. Jpn. **75**, 623 (2002).
[39] Y. Mizutani, Y. Uesugi, and T. Kitagawa, J. Chem. Phys. **111**, 8950 (1999).
[40] Y. Mizutani and T. Kitagawa, J. Mol. Liq. **90**, 233 (2001).
[41] Y. Mizutani and T. Kitagawa, Bull. Chem. Soc. Jpn. **75**, 965 (2002).
[42] Y. Zhang, H. Fujisaki, and J. E. Straub, J. Chem. Phys. **130**, 025102 (2009).
[43] H. Fujisaki, Y. Zhang, and J. E. Straub, J. Chem. Phys. **124**, 144910 (2006).
[44] N. Matsuzawa, M. Ata, and D. A. Dixon, J. Phys. Chem. **99**, 7698 (1995).
[45] D. R. Evans, T. Drovetskaya, R. Bau, C. A. Reed, and P. D. W. Boyd, J. Am. Chem. Soc. **119**, 3633 (1997).
[46] M. J. Frisch, G. W. Trucks, H. B. Schlegel *et al.*,GAUSSIAN 03, Revision C.02, Gaussian, Inc., Wallingford, CT, 2004.
[47] H. Fujisaki, L. Bu, and J. E. Straub, Adv. Chem. Phys. **130**, 179 (2005).
[48] H. Fujisaki and G. Stock, J. Chem. Phys. **129**, 134110 (2008).
[49] K. Moritsugu, O. Miyashita, and A. Kidera, J. Phys. Chem. B **107**, 3309 (2003).
[50] G. S. Kachalova, A. N. Popov, and H. D. Bartunik, Science **284**, 473 (1999).
[51] J. Kuriyan, S. Wilz, M. Karplus, and G. A. Petsko, J. Mol. Biol. **192**, 133 (1986).
[52] See EPAPS Document No. E-JCPSA6-130-002910 for additional data tables. For more information on EPAPS, see http://www.aip.org/pubservs/epaps.html.
[53] M. R. Armstrong, J. P. Ogilvie, M. L. Cowan, A. M. Nagy, and R. J. D. Miller, Proc. Natl. Acad. Sci. U.S.A. **100**, 4990 (2003).
[54] J. R. Hill, E. L. Chronister, T.-C. Chang, H. Kim, J. C. Postlewaite, and D. D. Dlott, J. Chem. Phys. **88**, 2361 (1988).
[55] A. Nitzan and J. Jortner, Mol. Phys. **25**, 713 (1973).